"A CMIP6 multi-model study of fast responses on pre-industrial climate due to present-day aerosols "

Prodromos Zanis[1], Dimitris Akritidis[1], Aristeidis K. Georgoulias[1], Robert J. Allen[2], Susanne E. Bauer[3], Olivier Boucher[4], Jason Cole[5], Ben Johnson[6], Makoto Deushi[7], Martine Michou[8], Jane Mulcahy[6], Pierre Nabat[8], Dirk Olivie[9], Naga Oshima[7], Adriana Sima[4], Michael Schulz[9], Toshihiko Takemura[10]

[1]Department of Meteorology and Climatology, School of Geology, Aristotle University of Thessaloniki, Thessaloniki, Greece
[2]Department of Earth Sciences, University of California Riverside, Irvine, USA
[3]NASA Goddard Institute for Space Studies, New York, USA
[4]CNRS, LMD/IPSL, Sorbonne Université, Paris, France
[5]Environment and Climate Change Canada, Toronto, Canada
[6]Met Office, Exeter, UK
[7]Meteorological Research Institute, Japan Meteorological Agency, Tsukuba, Japan
[8]CNRM, Université de Toulouse, Météo-France, CNRS, Toulouse, France
[9]Norwegian Meteorological Institute, Oslo, Norway
[10]Research Institute for Applied Mechanics, Kyushu University, Fukuoka, Japan

Co-financed by Greece and the European Union

Aim and data

To study the fast climate responses on pre-industrial climate, due to present-day aerosols.

Use Coupled Model Intercomparison Project Phase 6 (CMIP6) simulations from 10 Earth System Models (ESMs) and General Circulation Models (GCMs)

All models carried out two sets of simulations:

- A control experiment with all forcings set to the year 1850
- A perturbation experiment with all forcings identical to the control, except for aerosols with precursor emissions set to the year 2014.

Model	Resolution	Vertical levels	Model type	piClim-control Variant label	piClim-aer Variant label	piClim-SO_2 Variant label	piClim-BC Variant Label	piClim-OC Variant label	Reference/doi
CanESM5	2.8º x 2.8º;	49 levels; top level 1 hPa	ESM interactive chemistry	r1i1p2f1	r1i1p2f1				Cole et al., 2019a,b
CESM2	0.95º x 1.25º	32 levels; top level 2.25 hPa	ESM interactive aerosols	r1i1p1f1	r1i1p1f1				CESM2, 2018a,b
CNRM-CM6-1	1.4º x 1.4º	91 levels; top level 78.4 km	GCM no interactive aerosols	r1i1p1f2	r1i1p1f2				Voldoire, 2019a,b
CNRM-ESM2-1	1.4º x 1.4º	91 levels; top level 78.4 km	ESM fully interactive aerosols	r1i1p1f2	r1i1p1f2	r1i1p1f2	r1i1p1f2	r1i1p1f2	Seferian, 2019a,b Seferian et al., 2019 Michou et al., 2019
GISS-E2-1-G	2º x 2.5º	40 levels; top level 0.1 hPa	GCM no interactive aerosols	r1i1p1f1	r1i1p1f1				GISS, 2019a,b Kelley et al., 2020 Bauer and Tsigaridis, 2020
IPSL-CM6A-LR	1.27º x 2.5º	79 levels; top level 80 km	GCM prescribed aerosols	r1i1p1f1	r1i1p1f1				Boucher et al., 2018 Boucher et al., 2019
MIROC6	1.4º x 1.4º	81 levels; top level 0.004 hPa	GCM interactive aerosols	r1i1p1f1	r1i1p1f1				Sekiguchi and Shiogama~~Hideo~~, 2019a,b
MRI-ESM2-0	1.125º x 1.125º	80 levels; top level 0.01 hPa	ESM interactive aerosols	r1i1p1f1	r1i1p1f1	r1i1p1f1	r1i1p1f1	r1i1p1f1	Yukimoto et al., 2019a,b
NorESM2-LM	1.9º x 2.5º	32 levels; top level 3 hPa	ESM interactive aerosols	r1i1p1f1	r1i1p1f1	r1i1p1f1	r1i1p1f1	r1i1p1f1	NorESM2-LM, 2018a,b Kirkevåg et al., 2018
UKESM1-0-LL	1.25º x 1.875º	85 levels; top level 85 km	ESM interactive aerosols	r1i1p1f2	r1i1p1f2				O'Connor, 2019a,b

Table 1: Information on models resolution, vertical levels, model simulations and references.

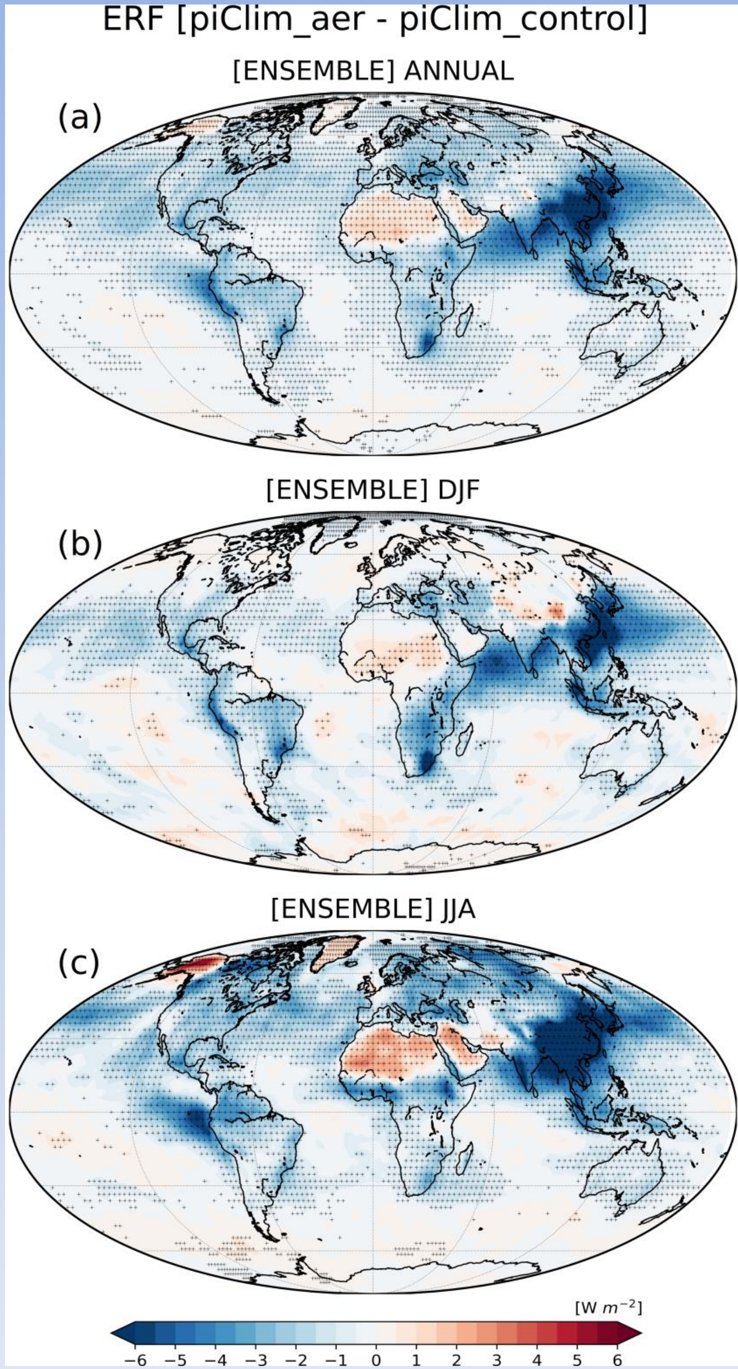

- The perturbation by the present-day aerosols indicates negative TOA ERF values around the globe, especially over continental regions of the Northern Hemisphere in summer, with the largest negative values over East Asia in response to the SO_2 emissions.

Figure 3: Differences between piClim-aer and piClim-control in the net radiative flux (W m^{-2}) at TOA including both SW and LW (all-aerosol ERF) for the ensemble of 10 models on an annual basis (a). for DJF (b) and for JJA (c). The dot shading indicates areas in which the differences are statistically significant at the 95% confidence level.

Source: Zanis et al., ACPD, https://doi.org/10.5194/acp-2019-1201

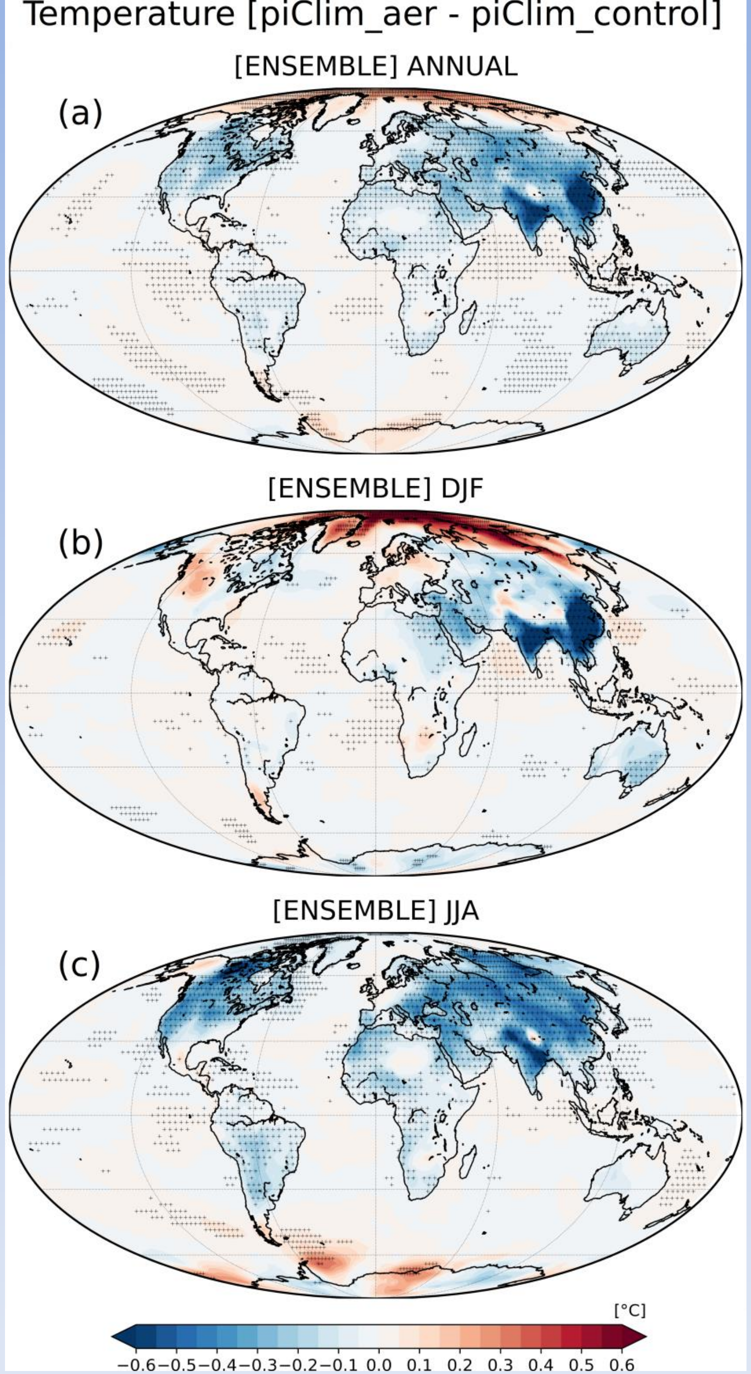

- The fast temperature responses are characterised by cooling over the continental areas, especially in the Northern Hemisphere with the largest cooling over East Asia and India.
- In the northern polar latitudes, there is a warming signal presumably linked to aerosol induced circulation changes

Figure 4: Differences between piClim-aer and piClim-control in near surface temperature (^{o}C) for the ensemble of 10 models on an annual basis (a). for DJF (b) and for JJA (c). The dot shading indicates areas in which the differences are statistically significant at the 95% confidence level.

Source: Zanis et al., ACPD, https://doi.org/10.5194/acp-2019-1201

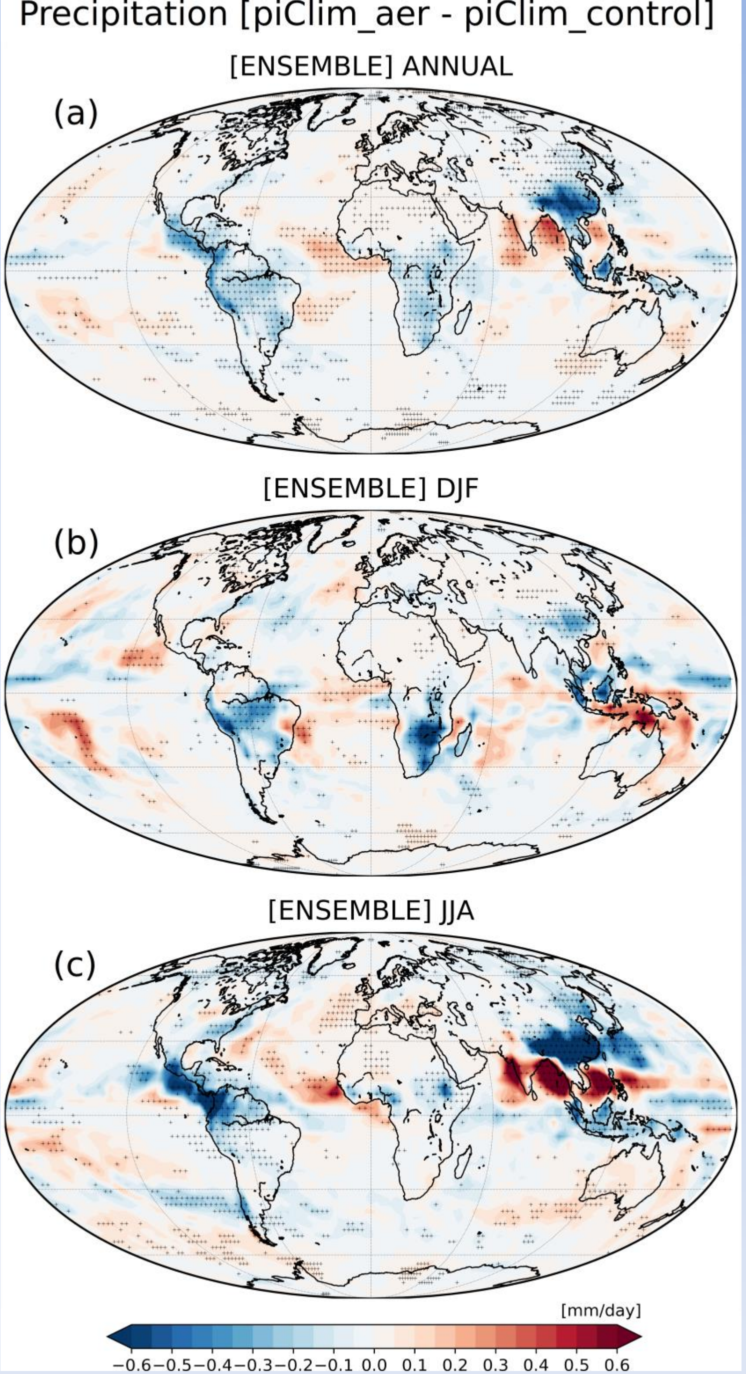

- There is dipole pattern of precipitation decrease over East Asia and increase over southern India, the Bay of Bengal and South China Sea. This is presumably associated to a southward shift of the ITCZ and weakening of the East Asia monsoon system.
- We also note a drying signal in Africa, shifting from Sahel in boreal summer JJA to southern Africa in austral summer DJF, linked possibly to a weakening of the West African and Southeast African monsoon systems.
- We note a drying signal in America, shifting from Central America in boreal summer JJA to South America in austral summer DJF, which is also associated with circulation changes inducing a weakening of the North American and South American Monsoon winds.

Figure 5: Differences between piClim-aer and piClim-control in precipitation (mm/day) for the ensemble of 10 models on an annual basis (a). for DJF (b) and for JJA (c). The dot shading indicates areas in which the differences are statistically significant at the 95% confidence level.

Source: Zanis et al., ACPD, https://doi.org/10.5194/acp-2019-1201

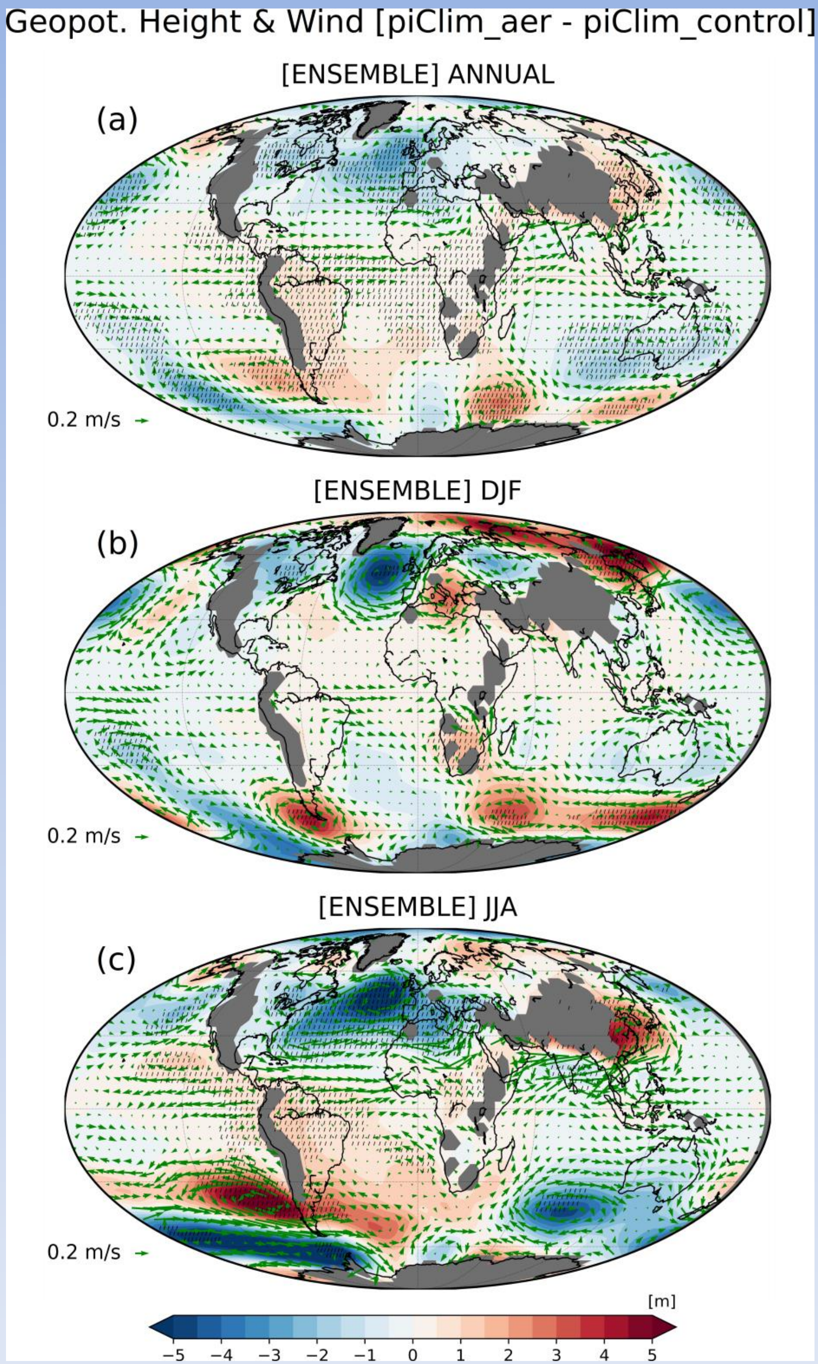

- An interesting feature in aerosol induced circulation changes is the characteristic dipole pattern with intensification of the Icelandic Low (cyclonic anomaly) and an anticyclonic anomaly over Southeastern Europe, inducing warm air advection towards the northern polar latitudes in DJF.

Figure 6: Differences between piClim-aer and piClim-control in geopotential height (m) and wind vectors at the 850 hPa pressure level for the ensemble of 10 models on an annual basis (a). for DJF (b) and for JJA (c). The dot shading indicates areas in which the differences are statistically significant at the 95% confidence level.

Source: Zanis et al., ACPD, https://doi.org/10.5194/acp-2019-1201

Key remarks

- The fast temperature responses are characterised by cooling over the continental areas, especially in the Northern Hemisphere, with the largest cooling over East Asia and India, sulfate being the dominant aerosol surface temperature driver for present-day emissions.
- The largest fast precipitation responses are seen in the tropical belt regions, generally characterized by a reduction over continental regions and a southward shift of the tropical rain belt.
- In the Arctic there is a warming signal for winter in the ensemble mean of fast temperature responses, but the model-to-model variability is large, and it is presumably linked to aerosol induced circulation changes with warm air advection towards the northern polar latitudes in winter.

Acknowledgments

Acknowledgements

We acknowledge support of this work by the project “PANhellenic infrastructure for Atmospheric Composition and climatE change” (MIS 5021516) which is implemented under the Action “Reinforcement of the Research and Innovation Infrastructure”, funded by the Operational Programme "Competitiveness, Entrepreneurship and Innovation" (NSRF 2014-2020) and co-financed by Greece and the European Union (European Regional Development Fund).

European Union
European Regional Development Fund
HELLENIC REPUBLIC
MINISTRY OF ECONOMY & DEVELOPMENT
SPECIAL SECRETARY FOR ERDF & CF
EPAnEK 2014-2020
OPERATIONAL PROGRAMME
COMPETITIVENESS ENTREPRENEURSHIP INNOVATION
ΕΣΠΑ 2014-2020
Partnership Agreement 2014-2020

Co-financed by Greece and the European Union